

Zero-dimensional modelling and bacterial characterization of an aerobic granular sludge reactor

Mario Plattes^{1*}, Xavier Goux¹, Oliver O’Nagy¹, Boris Untereiner¹,

¹ Luxembourg Institute of Science and Technology (LIST), Environmental Research and Innovation (ERIN), Site de Belvaux, 41 rue Brill, L-4422 Belvaux, Luxembourg

* Corresponding author: mario.plattes@list.lu

Abstract

A laboratory aerobic granular sludge (AGS) sequencing batch reactor (SBR) removing soluble organic substrate, nitrogen and phosphorous was fed with artificial wastewater and modelled using a zero-dimensional approach. Model development was supported by bacterial characterization using 16S rRNA gene amplicon high-throughput sequencing. The mathematical model was based on the activated sludge model nr. 2d (ASM2d) and extended with both two-step nitrification as implemented in the wastewater treatment plant simulator Sumo19 (Dynamita SARL) and ammonia nitrogen adsorption and desorption according to Langmuir. The model developed for the AGS was thus based on a model formulated for conventional activated sludge. The anaerobic filling and aerobic reaction phases were dynamically simulated. The mean simulated soluble chemical oxygen demand (11.0 mgCOD/l) was offset to the measured data (37.2 mgCOD/l). This was attributed to the formation of soluble microbial products, which were not considered in the model. The measured ammonia nitrogen, nitrite nitrogen, nitrate nitrogen, ortho-phosphate phosphorous, and dissolved oxygen concentrations were very well reproduced by the model (all Pearson’s r values ≥ 0.9479). However, anoxic (denitrification) processes by ordinary heterotrophic organism during the aeration phase had to be introduced, which underpinned the importance of anoxic zones in the granules under oxic bulk conditions.

Keywords

Aerobic granular sludge, biofilm, diffusion, half-saturation coefficient, modelling, Monod

1. Introduction

Aerobic granular sludge (AGS) has emerged as an advanced wastewater treatment technology and as a suppressing alternative to the conventional activated sludge (CAS) process [1]. This is because AGS has many advantages compared to CAS. In AGS the purifying biomass grows in compact cell aggregates that settle very fast and that feature stratification in aerobic, anoxic and anaerobic zones of the granules. The properties of AGS lead to a small footprint of the wastewater treatment plants (WWTPs) and small capital and operational expenses [2]. AGS technology as realized in sequencing batch reactors (SBRs) has the advantage that all processes can take place in one reactor and that there is no need for separate settlers and for recycle of sludge and wastewater as in CAS with secondary settlers.

AGS was first obtained at laboratory scale in a sequencing batch reactor (SBR) in 1997 [3]. The SBR was operated in cycles (fill, react, settle and draw) characterized by a very short settling time (≤ 1 min). This very short settling time resulted in the growth and selection of very fast settling granules in the reactor, i.e. slower settling aggregates were washed out whilst the granules were retained. Since then AGS is considered as a promising technology for wastewater treatment and as a major research topic. The research presented here develops on zero-dimensional (0D) mathematical modelling of AGS, i.e. not taking the structure of the granules into account.

Modelling can be a useful tool to describe and compile knowledge about AGS in a mathematical form. Ultimately, models can be used by practitioners for process design and optimization as demonstrated for CAS treatment by the state of the art activated sludge models (ASMs) from the ASM model family [4]. Note that AGS is seen as a biofilm system [5] and that biofilm models have first been used to mathematically describe the AGS system.

The first mathematical model of AGS grown in an SBR was proposed by Beun et al. [6]. This model was a one-dimensional (1D) model. It was implemented in AQUASIM, a simulator for aquatic systems [7]. The model used an extension of the biofilm model of Wanner & Gujer [8] as implemented in AQUASIM. However, the biofilm compartment in AQUASIM does not allow variable volumes and the model layout required the use of advective and diffusive links in order to implement the SBR. Following this concept, early AGS modelling was determined by the capacities of the

58 simulator AQUASIM, i.e. diffusive and/or advective links were needed in order to implement the variable volume of the
59 SBR. This AGS modelling concept, i.e. 1D with advective and diffusive links, has been adopted in further research, and
60 simulations have shown predictive power (see for example [9]).

61 More complex (2D and 3D) models have also been formulated for AGS [10-11]. As 1D models, these more complex
62 models simulate AGS structure and use *intrinsic* kinetic parameters; diffusion is modelled explicitly using Fick's laws.
63 Thus, in AGS modelling dimensional (1D, 2D, and 3D) biofilm models have been mainly used, because AGS is
64 considered to be a biofilm system (see [12] for a thorough review). In this research we elaborate on using the 0D modelling
65 approach with *extant* (apparent and measureable) kinetic parameters for modelling the AGS system.

66 Only one 0D AGS modelling study using ASM3 [4] is reported in early literature [13]. The 0D concept was demonstrated
67 in principle. However, the 0D approach was not further developed in the following years, and dimensional models have
68 pertained in AGS research. It was only recently that another 0D AGS model has been compared to a 1D model in a
69 simulation study [14] and it was found that the 0D model approximated the 1D model. Additionally it was demonstrated
70 in this study that this simple 0D (double Monod) model could dynamically predict real effluent ammonia nitrogen (NH₄-
71 N) concentrations of a full scale AGS plant.

72 Hence, although considerable research has been dedicated to AGS modelling, there is still a need to develop models of
73 the AGS process that adequately describe relevant processes and that can be used in engineering practice. This study aims
74 at further testing the 0D modelling approach for AGS in view of developing an AGS model for engineering practice. -
75 The 0D approach is encouraged by the previous development of a 0D biofilm model for dynamic simulation of moving
76 bed bioreactor (MBBR) systems [15] presented more recently elsewhere [16]. In order to do so, real data was collected
77 from a laboratory scale AGS SBR; the data was used to formulate the proposed 0D mathematical model. Simulation
78 results of unseen extend and quality (according to our knowledge) are presented, evaluated on real data, analysed and
79 discussed. This modelling study was complemented by microbiological characterization of the developed granules, which
80 was set into context of the mathematical modelling work.

81 82 83 **2. Materials and methods**

84 85 **2.1 Reactor operation and analysis**

86
87 The laboratory scale AGS reactor was based on the study of Beun et al. [6]: The reactor consisted of a transparent acrylic
88 glass tube (inner diameter = 6.2 cm, height = 120 cm, working volume = 3 dm³). The reactor was inoculated with activated
89 sludge from a dairy wastewater treatment plant that (biologically) removed COD, N, and P. The reactor was operated in
90 cycles using 60 min anaerobic fill (unmixed), 120 min react (aerated), 5 min settle, and 10 min decant. The reactor was
91 filled to a level of 100 cm and decanted from half the filling height, i.e. 50 cm (volume exchange ratio = 50 %). Aeration
92 was provided by an aquarium air pump (hygger) and an aeration stone. Wastewater was pumped in and out the reactor
93 using two peristaltic pumps (Thermo SCIENTIFIC, Masterflex P/S, Easy Load II). The aeration and peristaltic pumps
94 were controlled by an in house made control system using a Raspberry Pi and LABVIEW. The reactor was operated at
95 room temperature (23 ± 0.5°C).

96 Artificial wastewater was prepared in batches using commercially available chemicals (Fisher Scientific) with the
97 following concentrations: Sodium acetate (342 mgCOD/l), ammonium chloride (17.5 mgN/l), mono- and di-potassium
98 phosphate (3.3 mgP/l in total), magnesium sulfate heptahydrate (83 mg/l), and potassium chloride (33 mg/l). The
99 COD:N:P ratio was thus 100:5:1 in the artificial wastewater. A volume of 1.5 ml of trace element solution (adapted from
100 [17]) was added to a batch of 83 l of artificial wastewater prepared with tap water.

101 Standard wastewater components (COD, ammonium-N, nitrite-N, nitrate-N, and orthophosphate-P) were analysed using
102 cuvette tests (Hach). Wastewater samples were filtered through a 0.7 µm pore filter (WTW) before analysis. The dissolved
103 oxygen (DO) concentration was measured during the aerobic phase using a benchtop meter and an on-line probe (WTW,
104 inoLAB). A detailed analysis (sampling interval of 10 min during one aeration phase) of wastewater characteristics was
105 performed on operational day 367.

106 107 **2.2 Bacterial Characterization**

108
109 Granules were collected from the AGS reactor in order to evaluate their bacterial structure on operational day 368. For
110 that purpose, a volume of approximately 250 µL of AGS containing granules was sampled during the aeration phase and
111 directly frozen in liquid nitrogen. The frozen aliquots were stored at -80 °C prior to analysis. Before DNA extraction, the
112 sample was thawed, centrifuged for 15 min at 14 000 g, and supernatant was removed. DNA from the pellet (granules)
113 was extracted using the PowerSoil DNA Isolation kit (MoBio) according to the manufacturer's protocol. The bacterial
114 16S rRNA gene amplicon libraries were prepared as previously described (see [18] and references in there). Briefly, the
115 modified universal primer pair S-D-Bact-0909-a-S-18 and S*-Univ-*-1392-a-A-15 and Nextera XT Index Kit V2

(Illumina) were used along with Q5 Hot Start High-Fidelity 2x Master Mix (New England Biolabs) to perform two-step polymerase-chain reaction (PCR). In the first PCR, selective amplification of the 484 bp long fragments of bacterial 16S rRNA gene V6-V8 region was performed. In the second PCR, Illumina-compatible adapters and barcodes were attached to the previously amplified fragments. Purified libraries were sequenced along with PhiX control (Illumina) using Miseq Reagent Kit V3-600 on in-house Illumina MiSeq Platform. The sequencing results analysis (quality trimming, chimera check, singletons removal and assignment of the obtained sequences to operational taxonomic units (OTUs) at 97% similarity level) was done using usearch v11.0.667_i86linux64 software. The taxonomic affiliation of the resulting bacterial OTUs was performed using Mothur and SILVA database v.138. Most dominant OTUs were also taxonomically affiliated using the MiDAS database in order to get indication about their putative activity [19] and their closest cultivated sequences were determined using NCBI's BLAST and the refseq_rna database. The bacterial nucleotide sequences were deposited in the GenBank database under the accession numbers MZ410808 to MZ411347.

2.3 Modelling

The mathematical model of the AGS reactor was implemented in the wastewater treatment plant simulator Sumo19 (Dynamita SARL). The SBR object available in Sumo was used. This object/module is normally used to model SBRs with CAS. This SBR module has variable volume. The SBR was set-up as completely mixed during the fill and aeration phase. The mathematical model of the biochemical conversions behind this object was Sumo2, an activated sludge model based on ASM2d [4] and extended with two-step nitrification (see Sumo19 model sheet if available or contact Dynamita SARL for further information). The influent of the AGS reactor model was defined according to the composition of the artificial wastewater. The simulation was run over one filling and react phase; the settling and decant phases were not modelled. The initial amounts of active biomass, i.e. ordinary heterotrophic organisms (OHOs), phosphorous accumulating organisms (PAOs), ammonia oxidizing organisms (AOOs), and nitrite oxidizing organisms (NOOs) were estimated. Glycogen accumulating organisms (GAOs) were not considered. The author is aware that the estimates of active biomass are not absolute estimates since microbial activity is a product of amount of active biomass and specific growth rate, and depends of various environmental parameters. The respective specific growth rates were used with typical values used in ASM2d and Sumo2 ([4] and Sumo2 default values). Initial storage products were also estimated and some half-saturation coefficients and other parameters were calibrated (see 3.4 and Appendix I). Simulation results were evaluated by correlation with the measured data. Pearson's r values were calculated using the relevant dynamic data ranges (i.e. omitting concentrations that had become and stayed zero in the series).

3. Results and discussion

3.1 Reactor performance

The removal rates of chemical oxygen demand (COD), ammonium nitrogen ($\text{NH}_4\text{-N}$), and orthophosphate (PO-P) were excellent (Tab. 1). The soluble substrate (COD) was completely consumed before the beginning of the aeration phase (60 min) and it was assumed that the remaining COD was inert, because its amount did not further decrease during the aeration phase (60 – 180 min). This recalcitrant COD was attributed to the formation of soluble microbial products (SMP) as reported in the same range for AGS reactors in the literature [20]. Some nitrate nitrogen ($\text{NO}_3\text{-N}$) was found in the influent, which originated from the tap water. Also, a net production of $\text{NO}_3\text{-N}$ took place during the aeration phase due to nitrification; therefore the associated removal appeared with a negative value. The data set presented in table 1 was used for model calibration.

161 **Table 1:** Data set resulting from chemical analysis during one cycle of the AGS reactor and used for modelling.
 162

Sample Nr.	Time	COD	NH4-N	NO2-N	NO3-N	TIN	PO4-P
	[min]	[mg/l]	[mg/l]	[mg/l]	[mg/l]	[mg/l]	[mg/l]
Influent	0	340	17.9	0.091	4.07	22.061	3.76
0	60	39.9	6.5	0	2.34	8.84	32.6
1	70	32.5	4.62	0.299	2.55	7.469	27.9
2	80	35.1	2.72	0.671	2.65	6.041	25.5
3	90	41.4	0.809	1.07	4.46	6.339	19.2
4	100	48.4	0.16	0.751	5.55	6.461	14.4
5	110	21	0	0	5.86	5.86	10.7
6	120	40.6	0	0	6.02	6.02	6.75
7	130	26.4	0	0	5.94	5.94	4
8	140	46.7	0	0	5.97	5.97	2.71
9	150	34.9	0	0	5.73	5.73	1.26
10	160	57.3	0	0	5.94	5.94	0.602
11	170	21.9	0	0	5.96	5.96	0.301
12	180	37.5	0	0	5.94	5.94	0.313
Removal	[%]	89.0	100.0	100.0	-45.9	73.1	91.7

163
 164
 165 **3.2 Bacterial community structure of the granules**
 166

167 To characterise the bacterial structure of the granules developed in the studied AGS reactor, we sequenced the bacterial
 168 16S rRNA gene previously amplified of a sample of granules collected after 368 days of reactor operation. The high-
 169 throughput sequencing resulted in 114,135 reads, assigned to 584 bacterial OTUs (defined at 97 % sequence similarity).
 170 The calculated rarefaction curve reached a plateau (Figure 1c), indicating that most of the bacterial diversity was described
 171 by our sequencing. Indeed, the Boneh estimate indicates that no more than 28 OTUs (out of 584, *i.e.* less than 5 %) could
 172 have been additionally described by increasing the sequencing depth.

173 The studied aerobic granular sludge was mostly composed of bacteria affiliated to the phyla Proteobacteria (representing
 174 44.3 % of the total relative abundance), Bacteroidota (33.3% of the total relative abundance), Planctomycetota (8.4 % of
 175 the total relative abundance), and Chloroflexi (4.4 % of the total relative abundance) (Figure 1a). Organisms affiliated to
 176 other phyla such as Acidobacteriota, Myxococcota, Nitrospirota, Verrucomicrobiota for example represented less than 10
 177 % of the whole bacterial community in terms of relative abundance. This observation is consistent with the current
 178 knowledge on granular sludge in which Proteobacteria and Bacteroidota are found to be the dominant phyla (see for
 179 example [21]).
 180

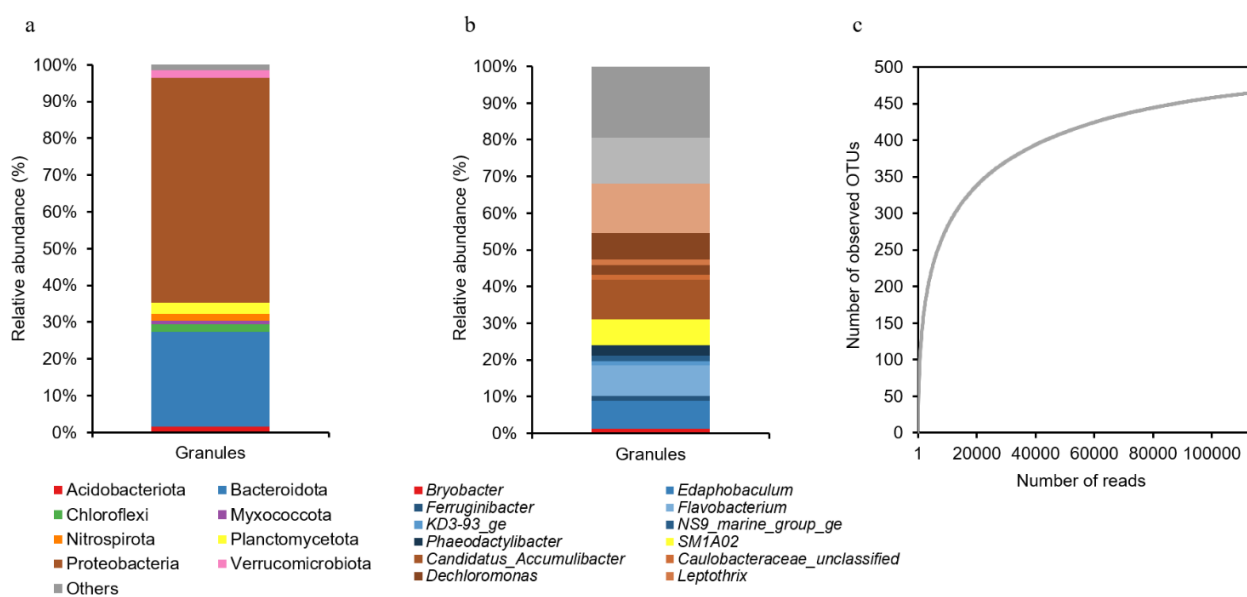


Figure 1:

Bacterial structure of the granules sampled in the studied AGS. Results are presented at the phylum level (a) and at the genus level (b). Panel c shows the observed richness estimator rarefaction curve of the high-throughput amplicon sequencing of the bacterial 16S rRNA gene for the analysed AGS sample.

207 **Table 2:** Phylogenetic affiliation and closest cultivated species of the 18 OTUs having a relative abundance above 1% in the studied granules

OTUs	Relative abundance (%)	Phylogenetic affiliation ^a			Closest cultivated species ^b		
		Phyla level	Genus level	Putative function	Specie name	Accession n.	Score (% identity)
Otu1	12.38	Proteobacteria	<i>Zoogloea</i>	OHO	<i>Zoogloea caeni</i>	NR_043795.1	100.00
Otu2	10.74	Proteobacteria	<i>Candidatus Accumulibacter</i>	PAO	<i>Propionivibrio pelophilus</i>	NR_024855.1	97.42
Otu3	8.27	Bacteroidota	<i>Flavobacterium</i>	OHO	<i>Flavobacterium keumense</i>	NR_157621.1	98.92
Otu10	7.29	Proteobacteria	<i>Thauera</i>	OHO	<i>Thauera aminoaromatica</i>	NR_027211.1	100.00
Otu5	4.96	Bacteroidota	<i>midas_g_729</i>		<i>Taibaiella yonginensis</i>	NR_145567.1	88.75
Otu4	4.94	Bacteroidota	<i>Taibaiella</i>		<i>Mucibacter soli</i>	NR_165710.1	94.68
Otu9	3.85	Chloroflexi	<i>Candidatus Villigracillis</i>		<i>Bellilinea caldifistulae</i>	NR_041354.1	92.51
Otu12	3.64	Planctomycetota	<i>SM1A02</i>		<i>Phycisphaera mikurensis NBRC 102666</i>	NR_074491.2	86.97
Otu14	3.12	Planctomycetota	<i>SM1A02</i>		<i>Thermogutta hypogea</i>	NR_134825.1	88.42
Otu7	3.00	Bacteroidota	<i>Phaeodactylibacter</i>	OHO	<i>Haliscomenobacter hydrossis</i>	NR_074420.1	95.46
Otu11	2.75	Proteobacteria	<i>Dechloromonas</i>	OHO	<i>Dechloromonas hortensis</i>	NR_042819.1	99.14
Otu8	2.18	Bacteroidota	<i>Ferruginibacter</i>		<i>Mucibacter soli</i>	NR_165710.1	95.11
Otu25	1.50	Proteobacteria	<i>Ideonella</i>	OHO	<i>Aquicola amnicola</i>	NR_159088.1	98.05
Otu26	1.32	Proteobacteria	<i>Caulobacter</i>		<i>Brevundimonas aveniformis</i>	NR_043770.1	99.78
Otu23	1.16	Bacteroidota	<i>Ferruginibacter</i>	OHO	<i>Ferruginibacter lapsinans</i>	NR_044589.1	97.01
Otu290	1.09	Proteobacteria	<i>Zoogloea</i>	OHO	<i>Zoogloea ramigera</i>	NR_113749.1	98.93
Otu30	1.06	Bacteroidota	<i>midas_g_3492</i>		<i>Tenacibaculum caenipelagi</i>	NR_125675.1	86.72
Otu29	1.04	Bacteroidota	<i>midas_g_3846</i>		<i>Sphingobacterium spiritivorum</i>	NR_113707.1	88.63
Total	74.32						

208

209 ^a Phylogenetic affiliation was performed using the MiDAS database. ^b Closest cultivated sequences were determined using NCBI's BLAST and the refseq_rna database.

210 OHO: ordinary heterotrophic organism; PAO: phosphorous accumulating biomass.

211

212

213 At the genus level (Figure 1b), *Zoogloea* was the dominant genus, representing 13.48 % of the whole bacterial community,
 214 followed by *Candidatus Accumulibacter* (10.74 %), *Flavobacterium* (8.37), *Edaphobaculum* (7.64 %), *Thauera* (7.29 %) and
 215 *SMIA02* (6.94%) for example. It is interesting to highlight the high percentage of uncultured (*i.e.* uncharacterised)
 216 organisms at this taxonomic level (12.52 %). The presence of members of the genus *Zoogloea* which form cell aggregates
 217 embedded in gelatinous matrices, called zoogloal matrices [22], and members of genus *Flavobacterium* which support
 218 the granules formation by the production of extracellular polymeric substances [23] are typical and logical for the studied
 219 environment (AGS).

220 At the OTU level, the bacterial community structure was dominated by only 18 OTUs having each a relative abundance
 221 above 1 % (Table 2). These 18 OTUs accounted for roughly 74 % of the total relative bacterial community abundance.
 222 Two OTUs out of the 18 had a relative abundance above 10 %. Otu1 was the most dominant one in the granules,
 223 representing around 12.38 % of the total bacterial community. This OTU was taxonomically affiliated to *Zoogloea caeni*
 224 sp. nov. (100 percent identity of the 16s rRNA gene sequence), a floc-forming bacterium isolated from activated sludge,
 225 and responsible for a quick reduction of nitrate to nitrite [24]. The second most abundant OTU, Otu2 representing 10.74
 226 % of the bacterial community of the studied granules, was affiliated to *candidatus Accumulibacter*. This bacterial group
 227 is known to be able to accumulate large amounts of intracellular polyphosphate [25]. No representative organism with a
 228 percentage identity of 100 % could be identified for this specific OTU. According to the MiDAS database used to identify
 229 putative functions of the main OTUs present in the studied granules, most of them are ordinary heterotrophic organisms
 230 which mediates the biological processes of COD removal and denitrification [26] (Table 2).

231 These results were taken into account as much as possible for the model development described below, bearing in mind
 232 that more than 12 % of the identified OTUs could not be classified at the genus level and that the organisms for which a
 233 putative function could be associated, are representing only 48 % in terms of relative abundance of the whole bacterial
 234 community of the studied granules. These made the microbiological data set rather incomplete and indicative only.

235

236 3.3 Model Development

237

238 In a preliminary modelling attempt Sumo2 (see 2.3) was used as implemented in the software Sumo19 for conventional
 239 activated sludge modelling. Two significant observations and interpretations were made:

240

241 1. The ammonia nitrogen concentration (NH₄-N) at the beginning of aeration phase (6.5 mgN/l) was smaller
 242 than expected from the dilution effect only (17.90 mgN/l * 0.5 = 8.95 mgN/l; volume exchange rate = 50
 243 %). This was explained by adsorption of ammonium nitrogen to the granules as proposed in the literature
 244 [27].

245 2. The nitrate nitrogen concentration (NO₃-N) at the end of the aeration phase was much smaller than
 246 predicted by the model (data not shown). This was explained by the presence of anoxic zones in the granules
 247 during the aeration phase. (The simulation results could not be improved by adapting kinetic parameters
 248 sensibly in the model.)

249

250 Adsorption (Eq. 1) and desorption (Eq. 2) of ammonia nitrogen were therefore introduced according to Langmuir [28]. It
 251 was thus assumed that the ammonia nitrogen adsorption rate (r_{ads}) is proportional to the product of the adsorption rate
 252 constant (k_{ads}), the ammonia nitrogen concentration in the bulk (S_{NHx}), the concentration of adsorbed ammonia nitrogen
 253 at saturation ($S_{NHx,sat}$), and the relative amount of available adsorption sites, given by 1 minus the concentration of
 254 adsorbed ammonia nitrogen ($S_{NHx,ads}$) divided by the concentration of adsorbed ammonia nitrogen at saturation ($S_{NHx,sat}$).
 255 The desorption rate (r_{des}) was assumed to be proportional to the product of the desorption rate constant (k_{des}), the
 256 concentration of adsorbed ammonia nitrogen at saturation ($S_{NHx,sat}$), and the relative coverage.

257

258

$$259 \quad r_{ads} = k_{ads} \cdot S_{NHx} \cdot S_{NHx,sat} \cdot \left(1 - \frac{S_{NHx,ads}}{S_{NHx,sat}}\right) \quad Eq. 1$$

260

261

$$262 \quad r_{des} = k_{des} \cdot S_{NHx,sat} \cdot \left(\frac{S_{NHx,ads}}{S_{NHx,sat}}\right) \quad Eq. 2$$

263

264 Two new processes, two new parameters and one new state variable were thus added to Sumo2. The stoichiometric factors
 265 for the conversions between S_{NHx} and $S_{NHx,ads}$ were set to 1 and -1 respectively. The concentration of adsorbed ammonia
 266 nitrogen at saturation ($S_{NHx,sat}$) was assumed to be a constant, because the amount of biomass in the reactor, and hence the
 267 number of adsorption sites did not change significantly during a phase.

268
 269 The model matrix was further changed by emphasizing anoxic processes of ordinary heterotrophic organisms (OHOs)
 270 during the aeration phase. Note that denitrification by phosphorous accumulating organisms (PAOs) was “switched off”
 271 by setting the reduction factor for anoxic growth of these organisms to 0, this was in the sense of the original ASM2 [4]
 272 and supported by numerous simulations (data not shown).

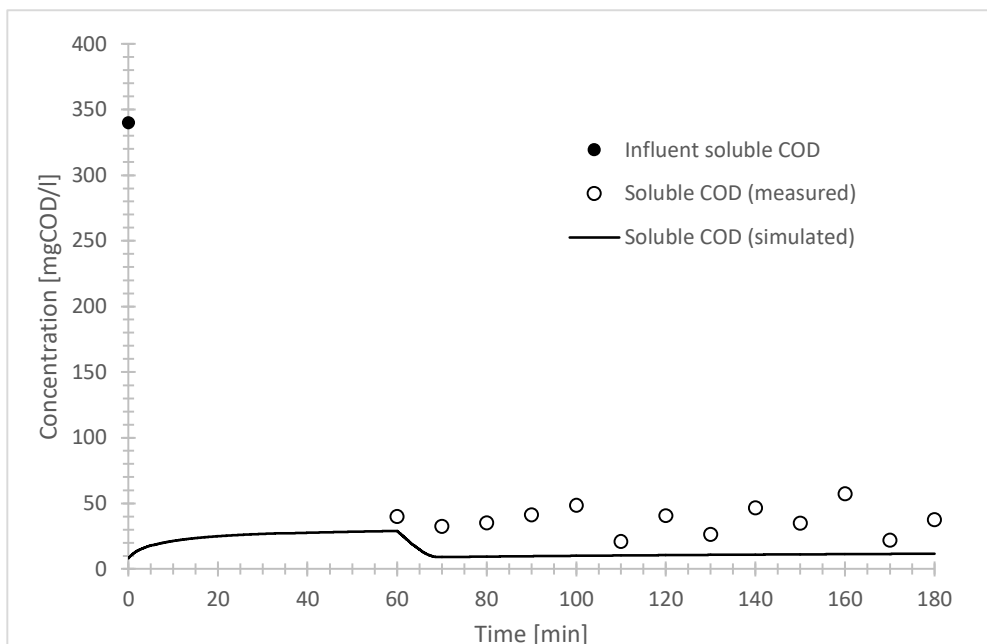
273 In order to do so, inhibition functions related to the bulk oxygen concentration for anoxic growth of OHOs were removed.
 274 As a result, anoxic growth could take place under aerobic bulk conditions. An inhibition function related to the bulk
 275 oxygen concentration for oxic growth of OHOs was introduced. As a result, this aerobic growth of OHOs did not take
 276 place under aerobic bulk conditions, and the organic substrate remained available for denitrification.

277
 278 Glycogen accumulating organisms (GAOs) were not considered in the model and their concentration was set to 0, because
 279 this organism group was not evidenced by the sequencing analysis (Table 2) and because all the organic substrate was
 280 taken up by PAOs. (GAOs will more likely have to be considered in AGS reactors fed with real wastewater.)

282 3.4 Calibration and simulation Results

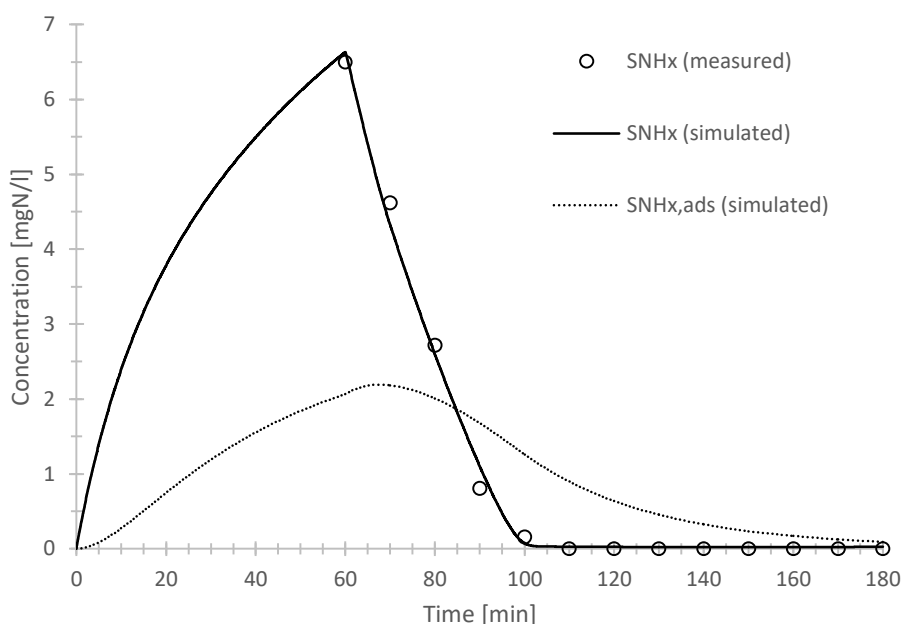
283
 284 During calibration, the initial amounts of active biomass, i.e. ordinary heterotrophic organisms (OHOs), phosphorous
 285 accumulating organisms (PAOs), ammonia oxidizing organisms (AOOs), and nitrite oxidizing organisms (NOOs) were
 286 estimated using the results presented in Table 1 and the charts presented below (Fig. 3-6). An overview of these and other
 287 estimated parameters can be found in Appendix I.

288
 289 The (soluble) chemical oxygen demand (*COD*) fluctuated during the aerobic reaction phase of the AGS reactor (Fig. 2);
 290 no continuous decline of this wastewater component could be observed. The mean value was found to be 37.2 mgCOD/l
 291 with a standard deviation of 10.4 mgCOD/l. This indicated that the soluble COD during the aerobic reaction phase was
 292 inert (as mentioned above) and originated from soluble microbial products (SMP). This inert COD did not originate from
 293 EDTA of the trace solution, that was added to the artificial wastewater only, and which had a final concentration of 1.8
 294 mg/l (i.e. 1.9 mgCOD/l), in the influent. However, formation of SMP was not modelled. This result meant that the soluble
 295 substrate provided as acetate was almost completely stored as polyhydroxyalkanoate (PHA) by the phosphorous
 296 accumulating organisms (PAOs) during the anaerobic feeding of the reactor. Some influent soluble substrate might also
 297 have been consumed by denitrifying biomass during anaerobic feeding, since nitrate nitrogen (NO₃-N) available from
 298 the influent (4.07 mgN/l), which was prepared with tap water, was slightly reduced after the anaerobic reaction phase
 299 (Fig. 4).



300
 301 **Figure 2:** Measured and simulated soluble COD concentrations in the influent and the AGS reactor.
 302
 303

304 The ammonium nitrogen concentration in the bulk (NH_4-N called $SNHx$ in the model) dropped from 17.9 mgN/l in the
 305 influent to 6.5 mgN/l at the beginning of the aerobic reaction phase, i.e. after 60 min anaerobic feeding (measured data in
 306 Fig. 3). As mentioned before, this was explained by dilution of the influent (volume exchange rate 50 %) and adsorption
 307 of ammonium nitrogen by the granules as proposed in the literature (Bassin *et al.* 2011). It was thus suggested, that 2.4
 308 mgN/l were adsorbed by the granules. This value seems to be plausible according to the literature (Bassin *et al.* 2011).
 309 Indeed, the model predicted an adsorbed ammonia nitrogen concentration ($SNHx_{ads}$) of 2.1 mgN/l at the beginning of
 310 the aeration phase (Fig. 3). It is further suggested, that the “missing” 0.3 mgN/l were taken up as nutrient by the biomass
 311 (OHOs and PAOs). The initial amount of AOOs was estimated to be 80 mgCOD/l and the respective half-saturation
 312 coefficient K_{NH_4} was set to 0.35 mgN/l. The default value for this parameter in ASMs is 1.00 mgN/l (Henze *et al.* 2000).
 313 This indicated that diffusion of ammonium nitrogen into the cell aggregate was less important for the aerobic granules
 314 than for typical conventional activated sludge, since diffusional mass transfer limitations manifest by increased half-
 315 saturation coefficients in activated sludge models [29-30].
 316



317
 318
 319 **Figure 3:** Measured and simulated ammonia nitrogen concentration in the bulk ($SNHx$), and (simulated) adsorbed
 320 ammonia nitrogen concentration ($SNHx_{ads}$) in the AGS reactor (Pearson's $r = 0.9971$).
 321

322 The measured nitrite nitrogen concentration (NO_2-N called SNO_2 in the model) during the aerobic reaction phase of the
 323 AGS reactor showed a peak (Fig. 4). The initial amount of NOOs was set to 50 mgCOD/l. The respective half-saturation
 324 coefficient was not changed. This peak was also well reproduced by the model. The nitrate nitrogen concentration (NO_3-
 325 N called SNO_3 in the model) at the beginning of the aerobic reaction phase (2.34 mgN/l) was well reproduced by the
 326 simulation (Fig. 4), but the subsequent increase of the measured data delayed relative to the simulated data. The authors
 327 have no explanation for this at the moment. The agreement of the simulation with the final measured nitrate nitrogen
 328 concentration was good. Overall it can be said that NO_2-N and NO_3-N were well reproduced by the model and
 329 quantitative agreement was found. Note that denitrification by PAOs was not considered by the model. Nitrite and nitrate
 330 depletion was thus due to anoxic growth of heterotrophic organisms only. This deserves further investigation..
 331

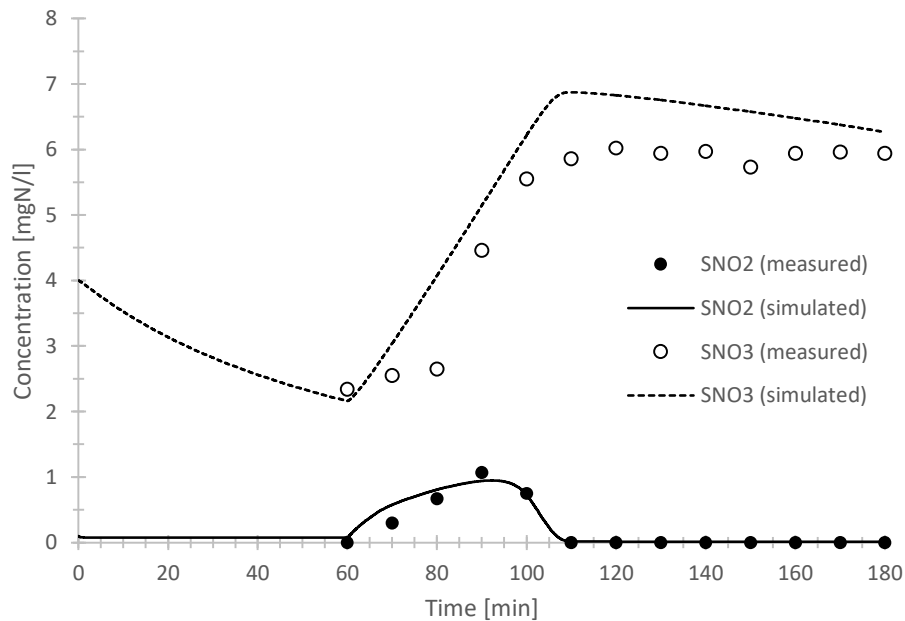


Figure 4: Measured and simulated NO₂-N (Pearson's $r = 0.9479$) and NO₃-N (Pearson's $r = 0.9716$) in the AGS reactor.

The total orthophosphate (**PO₄-P** called **SPO₄** in the model) release during the anaerobic feeding phase was well simulated by the model (Fig. 5). However, PO₄-P was not measured during anaerobic feeding, but the final PO₄-P concentration after feeding (32.6 mgP/l) was closely reproduced by the model. The uptake of PO₄-P during the aerobic reaction phase was well simulated by the model (Fig. 5). The initial amount of PAOs was set to 2500 mgCOD/l, the initial amount of PHA was 200 mgCOD/l and the initial amount of polyphosphate (PP) was 250 mgP/l. The half saturation coefficient for P-uptake (K_{PS}) was set to 8.0 mgP/l. The typical value for K_{PS} is 0.2 mgP/l (Henze *et al.* 2000) or 0.5 mgP/l (in Sumo2). This indicated that diffusion of PO₄-P into the cell aggregate was much more important for the aerobic granules than for conventional activated sludge, since diffusional mass transfer limitations manifest by increased half-saturation coefficients in activated sludge models [29-30].

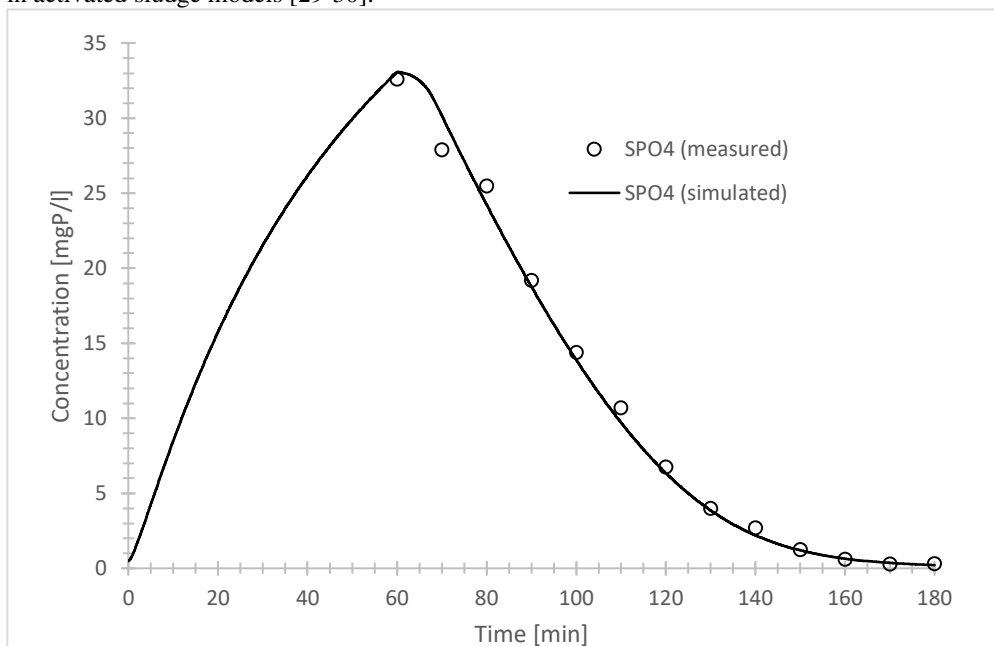
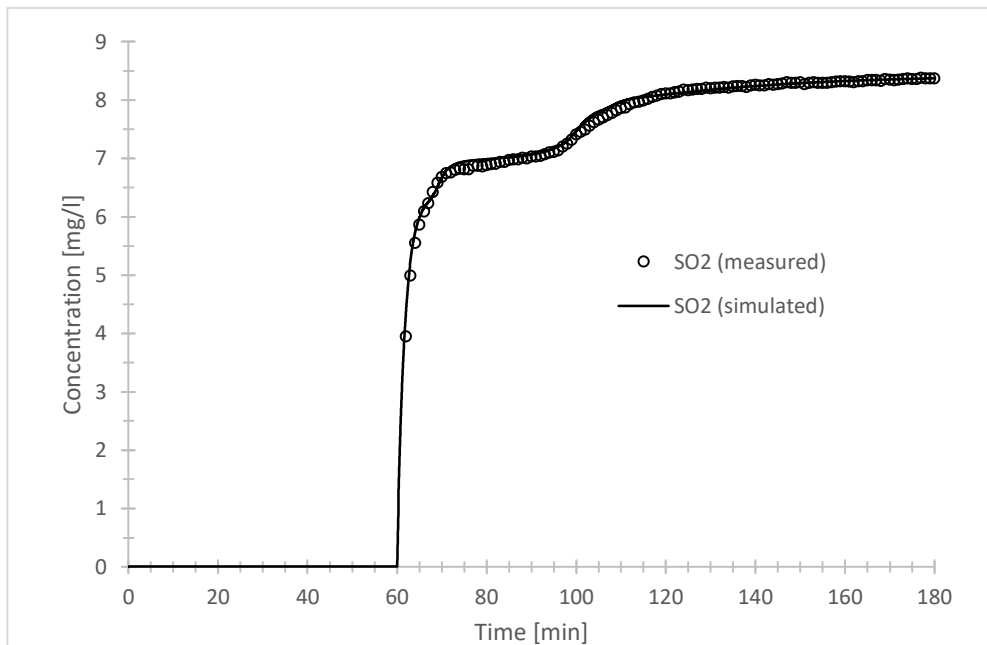


Figure 5: Measured and simulated PO₄-P in the AGS reactor (Pearson's $r = 0.9976$).

349
350
351
352
353

The dissolved oxygen concentration (*DO* called *SO₂* in the model) featured several bends which were very well reproduced by the model (Fig. 6). The air flow was estimated in the model to be 1.8 m³/d. The resulting oxygen mass transfer coefficient (*K_La*) was 827 1/d.



354
355
356
357
358
359
360
361
362
363
364
365
366

Figure 6: Measured and simulated DO in the AGS reactor (Pearson's $r = 0.9978$).

OHOs and PAOs were found to be the dominant species in the model, which corroborated the microbiological characterization of the granules. However, the relative abundance (expressed genetically) did not correspond to the relative amounts (expressed in biomass) found in the model. The authors think that this is because both measures cannot be directly correlated, and there are to the authors knowledge no correlation factors available in the literature. Further kinetic activity can be affected by various factors (e.g. temperature and pH) which might boost or impede activity of specific organism groups differently, thereby making a direct link of both measures difficult.

4. Conclusions

The zero-dimensional (0D) modelling approach was taken to model an AGS system fed with artificial wastewater and removing (soluble) COD, N, and P. The simulation results were very good for all reactants, i.e. COD, NH₄-N, NO₂-N, NO₃-N, PO₄-P, and DO. Anoxic (denitrification) processes during the aeration phase were introduced. This underpinned the presence and importance of relatively large anoxic zones in the granules during oxic bulk conditions.

This modelling approach deserves further testing with reactors fed with real wastewater, also on pilot and full scale, in order to confirm the applicability in engineering practice. The results are very promising and the 0D modelling approach offers an alternative to more complex dimensional (biofilm) models that emphasize cell aggregate structure. The authors believe that the research presented here will contribute to filling the gap that has developed over the past decades between dimensional biofilm research and engineering practice in the wastewater treatment modelling community.

376
377
378
379

Acknowledgements

The first author thanks Imre Takács and Dynamita SARL for providing a free trial license of Sumo19 and for giving technical support. The comments on a first manuscript draft by Mark van Loosdrecht were also highly appreciated. The authors acknowledge funding by the Ministry of Higher Education and Research (Luxembourg).

383
384
385

References

- 386
387
388 [1] J.P. Bassin, Aerobic Granular Sludge Technology, in: M. Dezotti, G. Lippel, J.P. Bassin (Eds.), *Advanced*
389 *Biological Processes for Wastewater Treatment – Emerging, Consolidated Technologies and Introduction to*
390 *Molecular Techniques*, Springer International Publishing, 2018, pp. 75-142.
- 391 [2] M. Pronk, M.K. de Kreuk, B. de Bruin, P. Kamminga, R.V. Kleerebezem, M.C.M. van Loosdrecht, Full scale
392 performance of the aerobic granular sludge process for sewage treatment, *Water Res.*, 84 (2015) 207-217.
393 <https://doi.org/10.1016/j.watres.2015.07.011>.
- 394 [3] E. Morgenroth, T. Sherden, M.C.M. van Loosdrecht, J.J. Heijnen, P.A. Wilderer, Aerobic granular sludge in a
395 sequencing batch reactor, *Water Res.*, 31(12) (1997), 3191-3194. [https://doi.org/10.1016/S0043-](https://doi.org/10.1016/S0043-1354(97)00216-9)
396 [1354\(97\)00216-9](https://doi.org/10.1016/S0043-1354(97)00216-9).
- 397 [4] M. Henze, W. Gujer, T. Mino, M.C.M. van Loosdrecht, *Activated Sludge Models ASM1, ASM2, ASM2d and*
398 *ASM3, IWA Task Group on Mathematical Modelling for Design and Operation of Biological Wastewater*
399 *Treatment* (ed.), Scientific and Technical Report No. 9, IWA Publishing, London, England (2000).
- 400 [5] J.J. Beun, M.C.M. van Loosdrecht, J.J. Heijnen, Aerobic granulation in a sequencing batch airlift reactor,
401 *Water Res.* 36 (2002) 702-712. [https://doi.org/10.1016/S0043-1354\(01\)00250-0](https://doi.org/10.1016/S0043-1354(01)00250-0).
- 402 [6] J.J. Beun, J.J. Heijnen, M.C.M. van Loosdrecht, N-Removal in a Granular Sludge Sequencing Batch Airlift
403 Reactor, *Biotechnol. Bioeng.*, 75(1) (2001), 82-92. <https://doi.org/10.1002/bit.1167>.
- 404 [7] P. Reichert, AQUASIM - A tool for simulation and data analysis of aquatic systems, *Water Sci. Technol.*,
405 30(2) (1994), 21-30. <https://doi.org/10.2166/wst.1994.0025>.
- 406 [8] O. Wanner, W Gujer, A Multispecies Biofilm Model, *Biotechnol. Bioeng.*, 28 (1986) 314-328.
407 <https://doi.org/10.1002/bit.260280304>.
- 408 [9] M.K. de Kreuk, C. Picoreanu, M. Hosseini, J.B. Xavier, M.C.M. van Loosdrecht, Kinetic Model of a
409 Granular Sludge SBR: Influence on Nutrient Removal, *Biotechnol. Bioeng.*, 97(4) (2007), 801-815.
410 <https://doi.org/10.1002/bit.21196>.
- 411 [10] J.B. Xavier, M.K. de Kreuk, C. Picoreanu, M.C.M. van Loosdrecht, Multi-Scale Individual-Based Model of
412 Microbial and Bioconversion Dynamics in Aerobic Granular Sludge, *Environ. Sci. Technol.*, 41(18) (2007),
413 6410-6417. <https://doi.org/10.1021/es070264m>.
- 414 [11] G.Q. Zheng, K.Z. Su, S. Zhang, Y.L. Wang, W.H. Wang, Three-dimensional multi-species mathematical
415 model of the aerobic granulation process based on cellular automata theory, *Water Sci. Technol.*, 77(12)
416 (2018), 2761-2771. <https://doi.org/10.2166/wst.2018.246>.
- 417 [12] J.E. Baeten, D.J. Batstone, O.J. Schraa, M.C.M. van Loosdrecht, E.I.P. Volcke, Modelling anaerobic,
418 aerobic and partial nitrification-anammox granular sludge reactors - A review, *Water Res.* 149 (2019) 322-341.
419 <https://doi.org/10.1016/j.watres.2018.11.026>.
- 420 [13] M. Lübken, N. Schwarzenbeck, M Wichern, P.A. Wilderer, Modelling nutrient removal of an aerobic granular
421 sludge lab-scale SBR using ASM3, in: S. Bathe, M. de Kreuk, B. McSwain, N. Schwarzenbeck (Eds.) *Aerobic*
422 *Granular Sludge*, IWA Publishing, London, UK, 2005, pp. .
- 423 [14] J. Baeten, M.C.M. van Loosdrecht, E.I.P. Volcke, Modelling aerobic granular sludge reactors through apparent
424 half-saturation coefficients. *Water Res.* 146 (2018) 134-145. <https://doi.org/10.1016/j.watres.2018.09.025>.
- 425 [15] M. Plattes, E. Henry, P.M. Schosseler, A zero-dimensional biofilm model for dynamic simulation of moving
426 bed bioreactor systems: Model concepts, Peterson matrix, and application to a pilot-scale plant, *Biochem. Eng.*
427 *J.* 40 (2008) 392–398. <https://doi.org/10.1016/j.bej.2008.01.011>.
- 428 [16] M. Plattes, Presentation and evaluation of the zero-dimensional biofilm model ODBFM, *Water Sci. Technol.*
429 79(1) (2019) 35-40.
- 430 [17] G.J.F. Smolders, J. van der Meij, M.C.M. van Loosdrecht, J.J. Heijnen, Stoichiometric Model of the Aerobic
431 Metabolism of the Biological Phosphorous Removal Process, *Biotechnol. Bioeng.* 44 (1994) 837-848.
432 <https://doi.org/10.1002/bit.260440709>.
- 433 [18] M. Calusinska, X. Goux, M. Fossépré, E.E.L. Muller, P. Wilmes, P. Delfosse, A year of monitoring 20
434 mesophilic full-scale bioreactors reveals the existence of stable but different core microbiomes in bio-waste
435 and wastewater anaerobic digestion systems, *Biotechnol. Biofuels* 11 (2018), 196.
436 <https://doi.org/10.1186/s13068-018-1195-8>.
- 437 [19] M. Nierychlo, K.S. Andersen, Y. Xu, N. Green, C. Jiang, M. Albertsen, M.S. Dueholm, P.H. Nielsen, MiDAS
438 3: An ecosystem-specific reference database, taxonomy and knowledge platform for activated sludge and
439 anaerobic digesters reveals species-level microbiome composition of activated sludge. *Water Res.*, 182 (2020)
440 115955. <https://doi.org/10.1016/j.watres.2020.115955>.
- 441 [20] L. Xi, D. Liu, W. Huang, Effect of acetate and propionate on the production and characterization of soluble
442 microbial products (SMP) in aerobic granular sludge system, *Toxicol. Environ. Chem.* 100(2) (2018) 175-190.
443 DOI:10.1080/02772248.2018.1493767.

- 444 [21] E. Szabó, R. Liébana, M. Hermansson, O. Modin, F. Persson, B.-M. Wilén, Microbial Population Dynamics
445 and Ecosystem Functions of Anoxic/Aerobic Granular Sludge in Sequencing Batch Reactors Operated at
446 Different Organic Loading Rates. *Front. Microbiol.* 8 (2017) 770. <https://doi.org/10.3389/fmicb.2017.00770>.
- 447 [22] P.R. Dugan, D.L. Stoner, H.M. Pickrum, The genus *Zoogloea*, in: A. Balows, H.G. Trüper, M. Dworkin, W.
448 Harder, K.-H. Schleifer (Eds.), *The Prokaryotes*, 2nd ed., Vol. III, New York, Springer, 1992, pp. 3952-3964.
- 449 [23] P. Swiatczak, A. Cydzik-Kwiatkowska, Performance and microbial characteristics of biomass in a full-scale
450 aerobic granular sludge wastewater treatment plant. *Environ. Sci. Pollut. Res.* 25(2) (2018) 1655-1669.
451 [10.1007/s11356-017-0615-9](https://doi.org/10.1007/s11356-017-0615-9).
- 452 [24] Y. Shao, B.S. Chung, S.S. Lee, W. Park, S.S. Lee, C.O. Jeon, *Zoogloea caeni* sp. Nov., a floc-forming
453 bacterium isolated from activated sludge. *Int. J. Syst. Evol.* 59 (2009) 526-530. [10.1099/ijs.0.65670-0](https://doi.org/10.1099/ijs.0.65670-0).
- 454 [25] S. He, K.D. Mc Mahon, Microbiology of *Candidatus Accumulibacter* in activated sludge, *Microbiol.*
455 *Biotechnol.*, 4(5) (2011) 603-619. [10.1111/j.1751-7915.2011.00248.x](https://doi.org/10.1111/j.1751-7915.2011.00248.x).
- 456 [26] B.J. Lee, M.C. Wentzel, G.A. Ekama, Measurement and modelling of ordinary heterotrophic organism active
457 biomass concentrations in anoxic/aerobic activated sludge mixed liquor, *Water Sci. Technol.* 54(1) (2006) 1-10.
458 [10.2166/wst.2006.365](https://doi.org/10.2166/wst.2006.365).
- 459 [27] J.P. Bassin, M. Pronk, R. Kraan, R. Kleerebezem, M.C.M. van Loosdrecht, Ammonium adsorption in aerobic
460 granular sludge, activated sludge and anammox granules. *Water Res.* 45 (2011) 5257-5265.
461 <https://doi.org/10.1016/j.watres.2011.07.034>.
- 462 [28] P. Atkins, J. De Paula, J. Keeler, *Atkins' physical chemistry* (11th ed.). Oxford University Press (2017).
- 463 [29] M. Beccari, A.C. Di Pinto, R. Ramadori, M.C. Tomei, Effects of dissolved oxygen and diffusion resistances on
464 nitrification kinetics. *Water Res.*, 26(8) (1992), 1099-1104. [https://doi.org/10.1016/0043-1354\(92\)90146-U](https://doi.org/10.1016/0043-1354(92)90146-U).
- 465 [30] K.H. Chu., H.M. van Veldhuizen, M.C.M. van Loosdrecht Respiriometric measurement of kinetic parameters:
466 effect of activated sludge floc size. *Water Sci. Technol.* 48 (2003) 61-68.
467
468
469
470
471
472
473
474
475
476
477
478
479
480
481
482
483
484
485

486 **Appendix I**

487
488 Initial conditions, kinetic parameters, common switches, stoichiometric yields, and ammonia
489 nitrogen adsorption parameters used in the model.
490

Initial conditions (state variables)			
Active biomass	Unit	Value	Default
Ordinary Heterotrophic organisms (OHOs)	[mgCOD/l]	500	-
Phosphorus accumulating organisms (PAOs)	[mgCOD/l]	2500	-
Glycogen accumulating organisms (GAOs)	[mgCOD/l]	0	-
Ammonia oxydizing organisms (AOOs)	[mgCOD/l]	80	-
Nitrite oxydizing organisms (NOOs)	[mgCOD/l]	50	-
Storage products	Unit	Value	Default
Stored polyhydroxyalkanoates (PHA)	[mgCOD/l]	200	-
Stored polyphosphate (PP)	[mgP/l]	250	-
Kinetic parameters			
Ordinary Heterotrophic organisms (OHOs)	Unit	Value	Default
Reduction factor for anoxic growth of OHOs	-	0.10	0.6 ¹
Phosphorus accumulating organisms (PAOs)	Unit	Value	Default
Reduction factor for anoxic growth of PAOs	-	0.00	0.66 ¹
Half-saturation of PO ₄ for PAOs	[mgP/l]	8.00	0.50 ¹
Ammonia oxydizing organisms (AOOs)	Unit	Value	Default
Half-saturation of NH _x for AOOs	[mgN/l]	0.35	0.70 ¹
Common switches	Unit	Value	Default
Half-saturation of NH _x as nutrient for biomass	[mgN/l]	0.000	0.005 ¹
Stoichiometric yields	Unit	Value	Default
Ratio of P released per VFA stored	[mgP/mgVFA]	0.25	0.65 ¹
Ammonia nitrogen adsorption	Unit	Value	Default²
Adsorption rate constant for total ammonia N	[mgN/l.d]	6.00	-
Desorption rate constant for total adsorbed ammonia N	[1/d]	50.00	-
Maximum concentration of adsorbed ammonia N	[mgN/l]	6.00	-

¹ Default value in Sumo19

² Not defined in Sumo19

491
492
493